Blind Carrier Phase Acquisition and Tracking for 8-VSB Signals

Jenq-Tay Yuan, *Senior Member, IEEE,* and Yong-Fu Huang

***Abstract*—A blind carrier phase derotator can be employed to correct and track carrier phase offset either before or after equalization in a blind adaptive receiver. This work proposes a computationally efficient blind carrier offset recovery algorithm for 8-vestigial side-band (8-VSB) signals by designing its cost function such that its cost surface has only two global minima without any undesirable local minima. Consequently, the proposed algorithm is not complicated by the possibility of a stochastic gradient descent (SGD) algorithm converging to a false local minimum, and global convergence can always be ensured. Moreover, the proposed algorithm can adopt a large step size in the transient period to accelerate the convergence speed along with a small step size in the convergence period to reduce the stochastic gradient noise.**

***Index Terms*—Blind Adaptive receiver, blind equalization, blind carrier phase recovery, constant modulus algorithm (CMA), decision-directed phase recovery (DDPR), digital television (DTV), dispersion minimization derotator (DMD), modified multimodulus algorithm (MMMA), multimodulus algorithm (MMA), stochastic gradient noise, 8-vestigial side-band (8-VSB).**

I. Introduction

BLIND adaptive equalization algorithms, such as the constant modulus algorithm (CMA), have been an active research topic over the last 25 years [1]-[4]. However, a *blind adaptive receiver* involves not only blind equalization to remove intersymbol interference (ISI), but also other important issues, such as carrier phase acquisition and tracking [5]. One way to deal with the phase recovery and tracking problems in high-speed synchronous digital communication systems, such as the large quadrature amplitude modulation (QAM) and 8-vestigial side-band (8-VSB) transmissions (Fig. 8 of [6]), is to employ a carrier phase derotator. The 8-VSB system has been adopted as the standard for digital television (DTV) broadcasting in the United States [6]-[8]. Therefore, developing computationally simple blind carrier phase derotators with guaranteed global convergence to correct and track carrier phase offset, either before or after blind equalization, is well motivated [9]. Chung, Sethares, and Johnson Jr. [7] proposed a dispersion minimization derotator (DMD) for blind adaptive carrier phase offset correction for both QAM and 8-VSB signals. However, this DMD scheme for 8-VSB signals produces undesirable local minima, leading to a slow convergence rate and high stochastic gradient noise. The decision-directed phase-recovery (DDPR) algorithm proposed by Chung *et al*. [10], [11] overcomes the problems of DMD, but may yield slow convergence in order to achieve reliable global convergence. This work proposes a computationally efficient blind carrier phase recovery algorithm, called the modified multimodulus algorithm (MMMA), for 8-VSB signals whose cost function can be designed to have only two global minima without any undesirable local minimum. The proposed cost surface thus ensures the global convergence. Moreover, the MMMA can automatically switch the step size in the stochastic update equation to yield fast convergence speed and low stochastic gradient noise. Notably, the MMMA proposed here is different from that proposed by He and Kassam in [12].

Consider a complex baseband VSB communication system in which s_n represents the complex 8-VSB signal at time n, which suffers from an unknown constant phase offset Φ in the presence of complex Gaussian noise w_n. Assuming that the timing recovery is perfect without any inter-symbol interference (ISI), the measured output, $y_n = s_n e^{j\Phi} + w_n$ is then sent to a single complex tap derotator intended to estimate Φ and remove this offset. The output of the complex one-tap blind carrier phase derotator, $f_n = r_n e^{j\phi_n}$, is then an estimate of the original transmitted data s_n and is given by $z_n = y_n f_n^* = r_n[s_n e^{j(\Phi-\phi_n)} + w_n e^{-j\phi_n}] = r_n[s_n e^{j\theta_n} + w_n e^{-j\phi_n}]$, where r_n is the magnitude of the single tap of the derotator; ϕ_n is an estimate of Φ and $\theta_n = \Phi - \phi_n$ is the phase estimation error (or parameter error). Our objective is to recover s_n from z_n by normalizing r_n once $\theta_n \to 0^\circ$ (or by normalizing r_n and then rotating by 90° or 270° once $\theta_n \to 90^\circ$ or $\theta_n \to 270^\circ$).

II. A Modified Multimodulus Cost Function

The cost function of the DMD proposed in [7] is given by

$$J_{DMD} = E\{[(\Re(y_n f_n^*))^2 - \gamma]^2\} \tag{1}$$

where $\Re(\cdot)$ denotes the real projection operator (i.e., $\Re(a + jb) = a$ and $\gamma = E[s_R^4]/E[s_R^2]$, in which s_R denotes the real part of s_n . The single tap-weight of the DMD is updated according to the stochastic gradient descent (SGD) algorithm

$$f_{n+1} = f_n - \mu[(\Re(y_n f_n^*))^2 - \gamma]\Re(y_n f_n^*) y_n \tag{2}$$

where μ is the step size. The DMD is based on the observation that Φ can be estimated by minimizing the dispersion of the projection of the VSB constellation onto the real axis. Although J_{DMD} for VSB in terms of both θ_n and r_n^2 yields two desired global minima at $\theta_n = 0^\circ$ and $\theta_n = 180^\circ$, it also yields two undesirable local minima at $\theta_n = 90^\circ$ and $\theta_n = 270^\circ$ (see Fig. 2(b) of [7]), which should be

Paper approved by C.-L. Wang, the Editor for Equalization of the IEEE Communications Society. Manuscript received November 26, 2008; revised June 29, 2009 and September 12, 2009.

J.-T. Yuan is with the Department of Electrical Engineering, Fu Jen Catholic University, Taipei 24205, Taiwan, R.O.C. (e-mail: yuan@ee.fju.edu.tw).

Y.-F. Huang was with the Department of Electrical Engineering, Fu Jen Catholic University, Taipei 24205, Taiwan, R.O.C.

This work was supported by the National Science Council (NSC), Taiwan, R.O.C. under contract NSC 98-2221-E-030-010-MY2. This paper was presented in part at the IEEE 13th International Symposium on Consumer Electronics, Kyoto, Japan, May 2009.

Digital Object Identifier 10.1109/TCOMM.2010.03.080624

avoided, since the large value of the DMD cost function at the two undesirable local minima, even in the absence of noise, produces large stochastic gradient noise [4, pp. 1941]. Moreover, the small values of curvature near the two undesirable local minima may slow down the convergence speed of the DMD.

A variant of DMD, called the multimodulus algorithm (MMA) [13]-[17], which was originally proposed to allow simultaneous joint blind equalization and carrier phase recovery in the field of blind equalization, can also be implemented with a single tap-weight as a blind carrier phase derotator [18], [19] with cost function

$$J_{MMA} = E\{[(\Re(y_n f_n^*))^2 - R_{2R}]^2\} + E\{[(\Im(y_n f_n^*))^2 - R_{2I}]^2\}$$

where $\Im(\cdot)$ denotes the imaginary projection operator (i.e., $\Im(a+jb) = b$), and R_{2R} and R_{2I} are given by $R_{2R} = E[s_R^4]/E[s_R^2]$ and $R_{2I} = E[s_I^4]/E[s_I^2]$, in which s_I denotes the imaginary part of s_n. This work proposes a modified version of MMA to estimate Φ with cost function

$$J_{MMMA} = N \cdot E\{[(\Re(y_n f_n^*))^2 - R_{2R}]^2\} + M \cdot E\{[(\Im(y_n f_n^*))^2 - R_{2I}]^2\} \quad (3)$$

where M and N are both real. J_{MMMA} in (3) can be designed to eliminate undesirable local minima, and to have a significantly reduced value at global minima, by choosing appropriate values for M and N such that the resulting algorithm, referred to as the *modified multimodulus algorithm (MMMA)*, always achieves global convergence with small stochastic gradient noise. The single tap-weight of the MMMA can be shown to be updated according to the SGD algorithm

$$f_{n+1} = f_n - \mu[N \cdot e_{R,n} - jM \cdot e_{I,n}] \cdot y_n \quad (4)$$

where $e_{R,n} = [(\Re(y_n f_n^*))^2 - R_{2R}] \cdot \Re(y_n f_n^*)$ and $e_{I,n} = [(\Im(y_n f_n^*))^2 - R_{2I}] \cdot \Im(y_n f_n^*)$.

For simplicity, additive channel noise w_n is set to zero in the following analysis. The derotator output can thus be expressed as

$$y_n f_n^* = (s_R r_n \cos\theta_n - s_I r_n \sin\theta_n) + j(s_R r_n \sin\theta_n + s_I r_n \cos\theta_n)$$

For notational simplicity, the time index, n, in the subscript may be dropped in the sequel, e.g., $\theta = \theta_n = \Phi - \phi_n = \Phi - \phi$. Substituting yf^* into J_{MMMA} in (3) yields

$$J_{MMMA} = N \cdot E\{[(s_R r\cos\theta - s_I r\sin\theta)^2 - R_{2R}]^2\} + M \cdot E\{[(s_R r\sin\theta + s_I r\cos\theta)^2 - R_{2I}]^2\}$$

For VSB signals, $E[s_R^2 s_I^2] = E[s_R^2]E[s_I^2]$ and $E[s_R^2] = E[s_I^2]$ can be obtained [7]. By setting $E[s_R^4] = m_{4R}$, $E[s_I^4] = m_{4I}$, $E[s_R^2] = E[s_I^2] = m_2$, $k_{SR} = m_{4R}/m_2^2$, and $k_{SI} = m_{4I}/m_2^2$, after some algebraic manipulations, the MMMA cost function can therefore be expressed as

$$J_{MMMA} = N \cdot \{m_2^2 k_{SR} r^4 \cos^4\theta + m_2^2 k_{SI} r^4 \sin^4\theta + \frac{3}{2} m_2^2 r^4 \sin^2 2\theta - 2R_{2R} m_2 r^2 + R_{2R}^2\} + M \cdot \{m_2^2 k_{SR} r^4 \sin^4\theta + m_2^2 k_{SI} r^4 \cos^4\theta + \frac{3}{2} m_2^2 r^4 \sin^2 2\theta - 2R_{2I} m_2 r^2 + R_{2I}^2\} \quad (5)$$

To obtain the stationary points of the MMMA, its cost function in (5) is differentiated with respect to θ , and then set to zero, yielding

$$\frac{\partial J_{MMMA}}{\partial\theta} = Nr^4 \sin 2\theta \cdot \{(6m_2^2 - 2m_{4R})\cos^2\theta + (2m_{4I} - 6m_2^2)\sin^2\theta\} + Mr^4 \sin 2\theta \cdot \{(2m_{4R} - 6m_2^2)\sin^2\theta + (6m_2^2 - 2m_{4I})\cos^2\theta\} = 0$$

Clearly, $m_{4R} \neq 3m_2^2$ and $m_{4I} \neq 3m_2^2$ for VSB signals, and, therefore, one set of stationary points of the MMMA cost function is at $\theta = 0°, 90°, 180°, 270°$ such that $\sin 2\theta = 0$. The other set of stationary points, which arises when $\sin 2\theta \neq 0$, can be obtained by solving

$$\cos^2\theta = \frac{N(3m_2^2 - m_{4I}) + M(3m_2^2 - m_{4R})}{(M+N)(6m_2^2 - m_{4R} - m_{4I})} \quad (6)$$

Notably, the MMMA is reduced to the DMD and the MMA, respectively, when $(M,N) = (0,1)$ and $(M,N) = (1,1)$. For the DMD case, substituting $(M,N) = (0,1)$ into (6) for 8-VSB yields $\theta = 60°, 120°, 240°, 300°$, which correspond to the four local maxima of the DMD cost function. For the MMA case, substituting $(M,N) = (1,1)$ into (6) for 8-VSB yields $\theta = 45°, 135°, 225°, 315°$, which correspond to the four local maxima of the MMA cost function.

To compute r at all the stationary points, the MMMA cost function is differentiated with respect to r and then set to zero, yielding

$$\frac{\partial J_{MMMA}}{\partial r} = 4r^3 m_2^2 [Nk_{SR}\cos^4\theta + Nk_{SI}\sin^4\theta + \frac{3}{2}N\sin^2 2\theta + Mk_{SR}\sin^4\theta + Mk_{SI}\cos^4\theta + \frac{3}{2}M\sin^2 2\theta] - 4rm_2(NR_{2R} + MR_{2I}) = 0 \quad (7)$$

Clearly, one stationary point is at $r = 0$. For $r > 0$, (7) yields

$$r^2 = \frac{NR_{2R} + MR_{2I}}{m_2[(Nk_{SR} + Mk_{SI})\cos^4\theta + (Mk_{SR} + Nk_{SI})\sin^4\theta + \frac{3}{2}(N+M)\sin^2 2\theta]} \quad (8)$$

Substituting $\theta = 0°, 90°, 180°, 270°$ into (8) yields

$$r^2 = \begin{cases} 1, & \text{for } \theta = 0° \text{ and } \theta = 180° \\ \frac{Nk_{SR} + Mk_{SI}}{Nk_{SI} + Mk_{SR}}, & \text{for } \theta = 90° \text{ and } \theta = 270° \end{cases} \quad (9)$$

which are the values of r^2 at the four stationary points of the MMMA, where M and N are real values to be determined. The following two cases summarize the locations of all the stationary points for DMD and MMA. (i) The DMD case (when $(M,N) = (0,1)$): For the four stationary points at $\theta = 0°, 90°, 180°, 270°$, r^2 is calculated from (9) as

$$r_{DMD}^2 = \begin{cases} 1, & \text{for } \theta = 0° \text{ and } \theta = 180° \\ \frac{k_{SR}}{k_{SI}} = 0.681, & \text{for } \theta = 90° \text{ and } \theta = 270° \end{cases}$$

where $R_{2R} = k_{SR} m_2 = m_{4R}/m_2$. For the stationary points at $\theta = 60°, 120°, 240°, 300°$, r^2 is calculated from (8) as $r_{DMD}^2 = 0.6549$. (ii) The MMA case (when $(M,N) = (1,1)$): For the four local maxima at $\theta = 45°, 135°, 225°, 315°$, r^2 is calculated from (8) as $r_{MMA}^2 =$

0.8405. For the four local minima at $\theta = 0°, 90°, 180°, 270°$ whose normalized cost can be computed to be $J_{MMA(min)} = 0.887$, r^2 is calculated from (9) as $r^2_{MMA} = 1$. The normalized cost functions described in this work involve dividing the original cost function by the cost at the local maxima. Owing to the large normalized cost at the local minima, MMA may yield a large stochastic gradient noise in the steady state, even though its global convergence is always guaranteed.

III. Modified Multimodulus Algorithm (MMMA)

To simplify the following derivation of the MMMA, $M = 1$ is set throughout the remainder of this work. The lower and upper bounds of N are chosen such that the undesirable local minima may be completely eliminated from the MMMA cost function, and the normalized cost of the MMMA at the global minima almost diminishes to zero, i.e., $J_{MMMA(min)} \cong 0$. First of all, from (9)

$$r^2 = \frac{Nk_{SR} + Mk_{SI}}{Nk_{SI} + Mk_{SR}} = \frac{Nk_{SR} + k_{SI}}{Nk_{SI} + k_{SR}} > 0, \text{for } \theta = 90° \text{ and } 270° \tag{10}$$

must be satisfied. For 8-VSB signals, substituting $k_{SR} = 1.7619$ and $k_{SI} = 2 + \frac{k_{SR}}{3} = 2.5873$ into (10) such that it satisfies both $Nk_{SR} + k_{SI} > 0$ and $Nk_{SI} + k_{SR} > 0$, which yields $N > -0.681$. Another possibility is that both $Nk_{SR} + k_{SI} < 0$ and $Nk_{SI} + k_{SR} < 0$, which yields $N < -1.468$. Therefore, we have

$$N > -0.681 \text{ or } N < -1.4684 \tag{11}$$

To compute the curvature at the four stationary points at $\theta = 0°, 90°, 180°, 270°$, the MMMA cost function is differentiated twice with respect to θ, to yield

$$\begin{aligned}\frac{\partial^2 J_{MMMA}}{\partial \theta^2} &= Nr^4 \cdot \{(6m_2^2 - 2m_{4R})(2\cos^2\theta\cos 2\theta - \sin^2 2\theta) \\ &\quad + (2m_{4I} - 6m_2^2)(\sin^2 2\theta + 2\sin^2\theta\cos 2\theta)\} \\ &\quad - Mr^4 \cdot \{(6m_2^2 - 2m_{4R})(\sin^2 2\theta + 2\sin^2\theta\cos 2\theta) \\ &\quad + (2m_{4I} - 6m_2^2)(2\cos^2\theta\cos 2\theta - \sin^2 2\theta)\}\end{aligned} \tag{12}$$

The following two conditions are considered: (i) The freedom of choosing N allows the two *local maxima* to be located at $\theta = 0°$ and $\theta = 180°$, i.e., $\frac{\partial^2 J_{MMMA}}{\partial \theta^2} < 0$ must be satisfied by substituting $r^2 = 1$ and $\theta = 0°$ (or $\theta = 180°$) into (12), yielding

$$N < -\frac{1}{3} \tag{13}$$

(ii) The freedom of choosing N enables the two *global minima* to be located at $\theta = 90°$ and $\theta = 270°$, i.e., $\frac{\partial^2 J_{MMMA}}{\partial \theta^2} > 0$ must be satisfied by substituting $r^2 = \frac{Nk_{SR} + k_{SI}}{Nk_{SI} + k_{SR}}$ and $\theta = 90°$ (or $\theta = 270°$), into (12), yielding

$$N > -3 \text{ and } N \neq -1.4684 \tag{14}$$

Although the curvature at $\theta = 90°$ (or $\theta = 270°$) for $-3 < N < -1.4684$ can be computed from (12) to be positive, it is too small to allow the MMMA to converge effectively to the global minimum at $\theta = 90°$ (or $\theta = 270°$). Therefore, the values of N in $-3 < N < -1.4684$ are not considered to be appropriate.

The final condition that must be satisfied is that the MMMA cost function must be greater than or equal to zero at $\theta = 90°$ and $\theta = 270°$, where the two global minima of the MMMA cost function are located. This condition can be ensured by substituting $r^2 = \frac{Nk_{SR} + k_{SI}}{Nk_{SI} + k_{SR}}$ for $\theta = 90°$ (or $\theta = 270°$) into (5) such that $J_{MMMA(min)} \geq 0$, thus yielding

$$N \geq -0.4441 \text{ or } -2.33 < N \leq -0.681 \tag{15}$$

Collecting our results in (11), (13), (14) and (15), the overall admissible range of values for N is $-0.4441 < N < -\frac{1}{3}$. When $(M, N) = (1, -0.333)$, the normalized MMMA cost at the two global minima can be computed from (5) to be $J_{MMMA(min)} \cong 0.33$. However, the two global minima of the normalized MMMA cost function are such that their cost is least, with $J_{MMMA(min)} \cong 0$, when $(M, N) = (1, -0.444)$, which values are therefore adopted as the values of M and N in the proposed MMMA, because a large cost at the two global minima is associated with increased excess asymptotic error levels when a non-vanishing-step-size SGD algorithm is used [4, pp. 1941]. Additionally, the choice of $N = -0.444$ from the range of all values, $-0.4441 < N < -1/3$, yields the largest curvature at the four stationary points at $\theta = 0°, 90°, 180°, 270°$, maximizing the rate of convergence of the MMMA. That the choice of $N = -0.444$ maximizes curvature is confirmed as follows. Let $M = 1$, $A = 6m_2^2 - 2m_{4R}$, and $B = 2m_{4I} - 6m_2^2$, where both A and B can be computed to be greater than zero for 8-VSB signal. Then, (12) can be written as

$$\begin{aligned}\frac{\partial^2 J_{MMMA}}{\partial \theta^2} &= Nr^4 \cdot \{A(2\cos^2\theta\cos 2\theta - \sin^2 2\theta) \\ &\quad + B(\sin^2 2\theta + 2\sin^2\theta\cos 2\theta)\} \\ &\quad - r^4 \cdot \{A(\sin^2 2\theta + 2\sin^2\theta\cos 2\theta) \\ &\quad + B(2\cos^2\theta\cos 2\theta - \sin^2 2\theta)\}.\end{aligned}$$

Consider the following two cases. (i) When $\theta = 0°$ and $\theta = 180°$, $\frac{\partial^2 J_{MMMA}}{\partial \theta^2} = 2ANr^4 - 2Br^4 < 0$. Clearly, the choice of $N = -0.444$ from the range $-0.4441 < N < -1/3$ yields the largest negative curvature. (ii) When $\theta = 90°$ and $\theta = 270°$, $\frac{\partial^2 J_{MMMA}}{\partial \theta^2} = -2BNr^4 + 2Ar^4 > 0$. Clearly, the choice of $N = -0.444$ from the range $-0.4441 < N < -1/3$ yields the largest positive curvature.

Furthermore, substituting $(M, N) = (1, -0.444)$ into (6) for 8-VSB signals yields $\cos^2\theta = 1.1492 > 1$, which reveals that the set of stationary points that satisfy (6) in the proposed MMMA disappears. Although the choice of the two global minima at $\theta = 90°$ and $\theta = 270°$ in the proposed MMMA cost function always results in a phase offset, this offset can be accounted for *a priori* by simply rotating the MMMA derotator outputs by $90°$ or $270°$ and then correcting their magnitudes by a normalization factor, $r = \sqrt{\frac{Nk_{SR} + k_{SI}}{Nk_{SI} + k_{SR}}} \cong 1.716$, and the MMMA can still function properly. Figure 1 plots the normalized cost function of the MMMA in (5) when $(M, N) = (1, -0.444)$. This figure indicates that r^2 increases from unity to around 2.944, which range is much larger than those of DMD and MMA, as the MMMA cost decreases from the local maxima at $\theta = 0°$ (or $\theta = 180°$) to the desired global minima at $\theta = 90°$ (or $\theta = 270°$). This unique feature of the

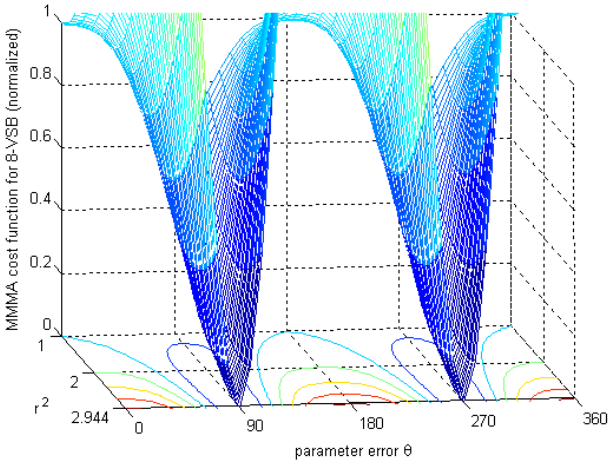

Fig. 1. Normalized cost function of MMMA for 8-VSB in terms of both r^2 and θ when $M = 1$ and $N = -0.444$.

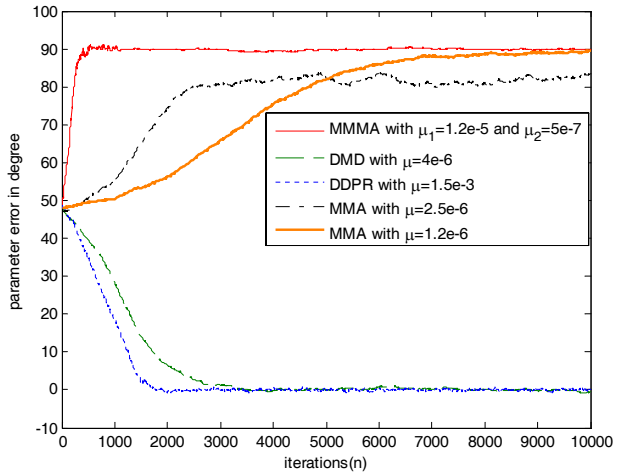

Fig. 2. Average trajectories of the parameter error $\theta_n = \Phi - \phi_n$ over 10 independent runs in terms of iterations, n, using MMMA, DMD, MMA, and DDPR with SNR = 20 dB for $\Phi = 48^\circ$.

MMMA cost function, along with $J_{MMMA(min)} \cong 0$, enables the following automatic switching of the step size to increase the convergence speed of the proposed MMMA in (4), while reducing the stochastic gradient noise.

The MMMA is implemented using (4) with two step sizes. Let a_n denote a flag that is set to be unity if $r_n^2 > 2.5$ (in the convergence period). Otherwise, let $a_n = 0$ (in the transient period). The automatic switching of the step size is described by the following formula similar to that of [20]. If $\sum_{i=0}^{L_1-1} a_{n-i} > \frac{L_1}{2}$, then set $\mu_2 = 5 \times 10^{-7}$, which is a small step size that is used to achieve a small mean-squared steady state error (or stochastic gradient noise), where $L_1 = 7$. Otherwise, set $\mu_1 = 1.2 \times 10^{-5}$, which is a large step size used to accelerate the convergence speed.

IV. Simulation Results

Chung [10] proposed a DDPR algorithm to overcome the problems of DMD. The cost function of DDPR is

$$J_{DDPR} = E\{[\Re(y_n f_n^*) - D(\Re(y_n f_n^*))]^2\}$$

where D denotes the decision device for 8-PAM. A normalized phase derotator (i.e., $r = 1$) update equation according to the SGD algorithm is given by

$$\phi_{n+1} = \phi_n + \mu[\Re(e^{-j\phi_n} y_n) - D(\Re(e^{-j\phi_n} y_n))]\Im(e^{-j\phi_n} y_n) \quad (16)$$

Similar to the DMD cost function, the DDPR cost function also yields two undesirable local minima at $\theta = 90^\circ$ and $\theta = 270^\circ$ [10], which should be avoided. To avoid these undesirable local minima, Chung developed the following global convergence control (GCC) that employs an adaptive monitoring device to determine when the derotator escapes the attraction region of the undesirable local minima.

$$r_{n+1} = r_n + \mu \mathcal{X}_y(y_n)[\Re(r_n y_n) - \Re(D(r_n y_n))]\Re(y_n) \quad (17)$$

where

$$\mathcal{X}_y(y_n) = \begin{cases} 1, & \text{if } |y_n| < 1.15 \\ 0, & \text{else} \end{cases} \quad (18)$$

The output of the adaptive monitoring algorithm is a correction of $\eta_n = 90^\circ$, which is subtracted from the parameter error θ once the DDPR is detected to be converging towards the undesirable local minima by utilizing

$$\eta_n = \begin{cases} 0, & \text{if } ||r_n| - 1| < \delta \\ 90^\circ, & \text{else} \end{cases} \quad (19)$$

Notably, (20) of [10] corresponding to (19) may have a typographical error. Although the DDPR with GCC always achieves global convergence and significantly reduces the stochastic gradient noise, the choice of both δ in (19) and the initial value of r_n (i.e., r_0) in (17) involves a trade-off between convergence speed and the reliability of global convergence. To achieve reliability, DDPR with GCC may result in slow convergence.

Simulation results of applying the MMMA, MMA, DMD and DDPR as blind carrier phase derotators for 8-VSB signals were compared. A single complex tap derotator, $f_n = r_n e^{j\phi_n}$, initialized as $f_0 = 1 + j0 = e^{j0}$, was employed to estimate Φ and remove this offset in the absence of the ISI in all four derotators. Figures 2 and 3 present the average trajectories of the parameter error $\theta_n = \Phi - \phi_n$ over 10 independent runs in terms of iterations, n, using MMMA with $(M, N) = (1, -0.444)$, DMD, MMA, and DDPR with signal-to-noise ratio $(SNR) = 20dB$ for $\Phi = 48^\circ$ and $\Phi = 70^\circ$, respectively, where $SNR = \frac{P_{avg}}{2\sigma_w^2}$, in which P_{avg} is the average power of the signal constellation and σ_w^2 is the variance of each component of the complex-valued white noise source. Notably, w_n is colored noise if the carrier phase derotator is used after equalization. However, the w_n used in the computer simulations was complex-valued white Gaussian noise.

Unlike DMD, MMA, and MMMA, the DDPR with GCC (with $\delta = 0.4$) in Fig. 3 exhibits a trajectory of only one single realization of parameter error θ_n, due to the difference in each realization as to when will the correction of 90° be made through the use of the GCC to escape the attraction of the undesirable local minima. The DMD algorithm was implemented using (2); the MMA was implemented using (4) with $(M, N) = (1, 1)$, and DDPR was implemented using

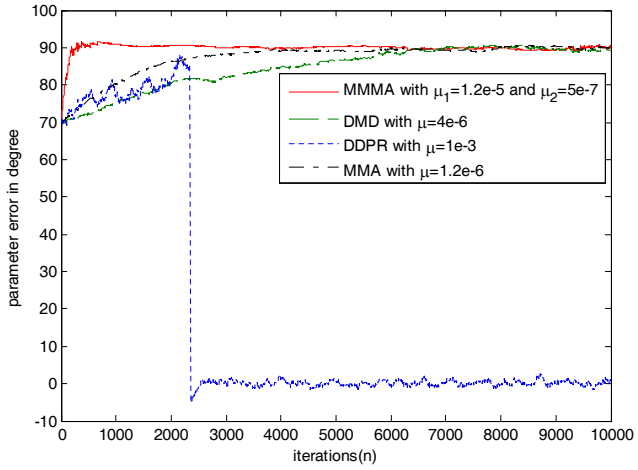

Fig. 3. Average trajectories of the parameter error $\theta_n = \Phi - \phi_n$ over 10 independent runs in terms of iterations, n, using MMMA, DMD, MMA, and DDPR (one single realization only) with SNR = 20 dB for $\Phi = 70°$.

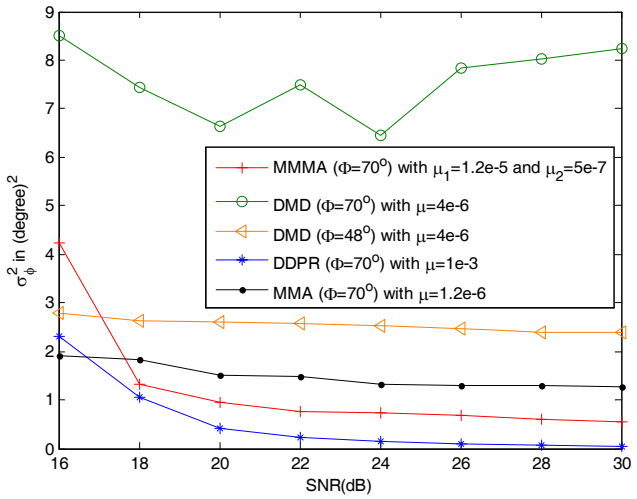

Fig. 4. Estimated mean-squared phase error versus SNR for various blind carrier phase derotators for 8-VSB signals.

(16) along with the GCC. Figure 4 compares the estimated mean-squared phase error, $\sigma_\phi^2 \approx E[(\Phi - \phi_n)^2]$, as a function of SNR for different carrier phase derotators with $\Phi = 70°$ (or $\Phi = 48°$). The estimated mean-squared phase error σ_ϕ^2 for each derotator was computed from the average of $(\Phi - \phi_n)^2$ from iteration $n = 9000$ to iteration $n = 10000$ over 20 independent runs for each given SNR. According to Fig. 2, the MMMA, DDPR, and DMD converged rapidly for $\Phi = 48°$. A relatively small step size $\mu = 1.2 \times 10^{-6}$ was required in the MMA to produce a small phase estimation error, owing to its large normalized cost at the global minima ($J_{MMA(min)} = 0.887$), but such a small step size reduced the convergence rate, as demonstrated in Fig. 2. For $\Phi = 70°$, Figs. 3 and 4 indicate that the DMD converged slowly to the undesirable local minimum at $90°$ where the stochastic gradient noise dominated, regardless of the SNR. The DDPR with GCC produced the smallest σ_ϕ^2 among the four derotators as shown in Fig. 4, but its convergence speed in Fig. 3 was not as fast as it was in Fig. 2, owing to the use of the GCC in Fig. 3 to avoid reaching undesirable local minima. The simulation results show that the average iteration at which a correction of $90°$ occurred was around the 2175^{th} iteration with a standard deviation of 706 iterations over 20 independent runs, when the DDPR was implemented with the GCC with $SNR = 20dB$ for $\Phi = 70°$. The proposed MMMA, given by (4), yielded rapid convergence with a relatively small stochastic gradient noise in Figs. 2-4, owing to its step size switching and its zero-cost minima. However, the MMMA exhibited a high σ_ϕ^2 when $SNR \leq 16dB$ because the large additive noise may have triggered the use of a large step size with $\mu = 1.2 \times 10^{-5}$ in the steady state, resulting in large stochastic gradient noise.

V. Conclusion

A blind carrier offset recovery algorithm for 8-VSB signals was proposed, with cost function $J_{MMMA} = N \cdot E\{[(\Re(y_n f_n^*))^2 - R_{2R}]^2\} + E\{[(\Im(y_n f_n^*))^2 - R_{2I}]^2\}$. The choice of $N = -0.444$ in J_{MMMA}, without producing any undesirable local minimum, is based on the following constraints. (a) The magnitude of the square of the single tap-weight of the proposed MMMA exceeds zero. (b) Two local maxima of the MMMA are located at $\theta = 0°$ and $\theta = 180°$, at which the largest possible negative curvature is produced. (c) Two global minima of the MMMA are located at $\theta = 90°$ and $\theta = 270°$, at which the largest possible positive curvature is produced. (d) The MMMA cost function produces the minimum cost $J_{MMMA(min)} \cong 0$ at the two global minima.

The MMMA cost function was initially designed such that the two global minima were set to $\theta = 0°$ and $\theta = 180°$ rather than $\theta = 90°$ and $\theta = 270°$, without any undesirable local minima, but the MMMA cost function prevented this aim from being realized. The proposed MMMA thus always requires a rotation by $90°$ (or $270°$) to correct the phase rotation. Nevertheless, the MMMA is computationally simple, and is demonstrated by simulations to exhibit fast convergence and generate small stochastic gradient noise in the steady state for moderate to high SNR's.

References

[1] J. R. Treichler, M. G. Larimore, and J. C. Harp, "Practical blind demodulators for high-order QAM signals," in *Proc. IEEE*, vol. 86, pp. 1907-1926, Oct. 1998.

[2] D. N. Godard, "Self-recovering equalization and carrier tracking in two-dimensional data communication system," *IEEE Trans. Commun.*, vol. 28, pp. 1867-1875, Nov. 1980.

[3] J. R. Treichler and M. G. Larimore, "New processing techniques based on the constant modulus algorithm," *IEEE Trans. Acoust., Speech, Signal Process.*, vol. ASSP-33, pp.420-431, Apr. 1985.

[4] C. R. Johnson, Jr., *et al.*, "Blind equalization using the constant modulus criterion: a review," *Proc. IEEE*, vol. 86, pp. 1927-1950, Oct. 1998.

[5] A. Belouchrani and W. Ren, "Blind carrier phase tracking with guaranteed global convergence," *IEEE Trans. Signal Process.*, vol. 45, pp. 1889-1894, July 1997.

[6] J. G. N. Henderson, *et al.* "ATSC DTV receiver implementation," *Proc. IEEE*, vol. 94, pp. 119-147, Jan. 2006.

[7] W. Chung, W. A. Sethares, and C. R. Johnson, Jr., "Performance analysis of blind adaptive phase offset correction based on dispersion minimization," *IEEE Trans. Signal Process.*, vol. 52, pp. 1750-1759, June 2004.

[8] M. Ghosh, "Blind decision feedback equalization for terrestrial television receivers," *Proc. IEEE*, vol. 86, pp. 2070-2081, Oct. 1998.

[9] E. Serpedin, P. Ciblat, G. B. Giannakis, and P. Loubaton, "Performance analysis of blind carrier phase estimators for general QAM constellations," *IEEE Trans. Signal Process.*, vol. 49, pp. 1816-1823, Aug. 2001.

[10] W. Chung, "Decision-directed carrier phase offset recovery scheme for 8-VSB signals," *IEEE Trans. Consumer Electron.*, vol. 53, pp. 1288-1292, Nov. 2007.

[11] W. Chung, *et al*., "A globally converging blind carrier phase offset recovery scheme for 8-VSB signals," in *Proc. Int. Conf. Consumer Electron.*, 2007, pp. 1-2.

[12] L. He and S. A. Kassam, "Convergence analysis of blind equalization algorithms using constellation-matching," *IEEE Trans. Commun*., vol. 56, pp. 1765-1768, Nov. 2008.

[13] K. Wesolowski, "Self-recovering adaptive equalization algorithms for digital radio and voiceband data modems," in *Proc. European Conf. Circuit Theory Design*, 1987, pp. 19-24.

[14] K. N. Oh and Y. O. Chin, "Modified constant modulus algorithm: blind equalization and carrier phase recovery algorithm," in *Proc. IEEE Int. Conf. Commun.*, 1995, pp. 498-502.

[15] J. Yang, J.-J. Werner, and G. A. Dumont, "The multimodulus blind equalization and its generalized algorithms," *IEEE J. Sel. Areas Commun.*, vol. 20, pp. 997-1015, June 2002.

[16] J.-T. Yuan and K.-D. Tsai, "Analysis of the multimodulus blind equalization algorithm in QAM communication systems," *IEEE Trans. Commun.*, vol. 53, pp. 1427-1431, Sept. 2005.

[17] J.-T. Yuan and T.-C. Lin, "Effect of source distributions on multimodulus blind equalization algorithm," in *Proc. 2008 IEEE Veh. Technol. Conf. (VTC)*, Spring 2008, pp. 668-672.

[18] H. Mathis, "Blind phase synchronization for VSB signals," *IEEE Trans. Broadcast.*, vol. 47, pp. 340-347, Dec. 2001.

[19] S. Abrar, "An adaptive method for blind carrier phase recovery in a QAM receiver," in *Proc. Int. Conf. Inf. Emerging Technol.*, 2007, pp. 1-6.

[20] K. Wesolowski, "Adaptive blind equalizers with automatically controlled parameters," *IEEE Trans. Commun*., vol. 43, pp. 170-172, Feb./Mar./Apr. 1995.